

## GROUND-SATELLITE STUDY OF A Pc 1 ION CYCLOTRON WAVE EVENT

B. J. Fraser, W. J. Kemp<sup>1</sup>, and D. J. WebsterDepartment of Physics, University of Newcastle  
New South Wales, Australia

**Abstract.** The magnetospheric generation and propagation characteristics of ion cyclotron waves associated with a Pc 1 emission observed by a network of four middle and low-latitude ground stations are determined using ground source location techniques and ISEE 1 plasma data. The source region at  $L = 4.7 \pm 0.7$  is determined from propagation in the  $F_2$  region ionospheric duct using wave polarization characteristics at ground stations. This source is just inside the steep plasmapause seen by ISEE 1 at  $L = 4.9 \pm 0.1$ . The ion cyclotron wave packet interhemispheric bounce period measured from the ground spectra increases with time from 140 to 155 s during the event but is in agreement with dispersion calculations undertaken using ISEE 1 electron density and cool to cold ion composition data in a  $H^+$  plasma with 8-10%  $He^+$  and <1%  $O^+$  ions. The frequency of the Pc 1 emission band seen on the ground (0.5-0.8 Hz) corresponds to the propagation region between the equatorial  $O^+$  cutoff frequency and the  $He^+$  cyclotron frequency. Linear convective growth rate calculations inside the plasmapause show significant wave amplitudes in this band. With these results it is possible to completely describe the wave generation mechanism and the magnetosphere ionosphere propagation characteristics for the Pc 1 event.

## Introduction

It is generally accepted that Pc 1 (0.2-5 Hz) geomagnetic pulsations observed on the ground are generated by an ion cyclotron resonance interaction in the magnetosphere between hydromagnetic waves and energetic protons [Mauk and McPherron, 1980; Roux et al., 1982]. The waves propagate as left-hand (LH) polarized ion cyclotron wave packets along field-aligned paths in the magnetosphere to the ionosphere where some of the energy is coupled to the right-hand (RH) mode and propagates by way of the  $F_2$  region ionospheric duct from the secondary source at the foot of the field line to higher and lower latitudes [Manchester, 1968]. The remaining energy is reflected back into the magnetosphere and gives rise to a wave packet bouncing between hemispheres.

<sup>1</sup>Now at CSIRO, Division of Environmental Mechanics, Institute of Physical Sciences, Canberra, Australian Capital Territory, Australia.

Copyright 1989 by the American Geophysical Union.

Paper number 89JA00924  
0148-0227/89/89JA-00924\$05.00

An important aspect of the theory of structured Pc 1 pulsations is the precise location of the region of generation and amplification and the associated L value of the field line along which the wave energy propagates. Theoretical studies of ion cyclotron instability processes [Kennel and Petschek, 1966; Criswell, 1969] suggest that the waves are generated in the equatorial  $L = 3-8$  region of the magnetosphere during the recovery phase of magnetic storms, when the plasmapause expands into the spatial region of the ring current. This suggests a source region in the vicinity of the plasmapause [Kawamura et al., 1982]. In addition, previous ground-based Pc 1 pulsation studies indicate sources in the region of  $L = 3-5$  and on or within the plasmapause [Fraser et al., 1984; Webster and Fraser, 1985]. This conclusion is supported by the absence of structured Pc 1 emissions at synchronous orbit ( $L = 6.6$ ) [Perraut, 1982] which is generally at a higher altitude than the plasmapause, except during the late afternoon and evening in the dusk bulge region. On the other hand, unstructured emissions characteristic of high latitudes on the ground are seen predominantly at synchronous orbit [Perraut et al., 1984].

Several experimental methods have been used to locate the source of structured emissions. These include the latitudinal and longitudinal distribution of signal amplitudes using a network of closely spaced stations below the high-latitude secondary source region [Hayashi et al., 1981]. Attempts to locate the source of individual structured Pc 1 events have included studies of the dispersion properties of ion cyclotron wave packets propagating along magnetospheric field-aligned paths [Gendrin et al., 1971, and references therein], studies of the wave packet bounce period with assumed cold plasma distribution and magnetic field models [Feigen et al., 1979], and polarization studies employing the principle that at large distances from the ionospheric source the major axis of a linear ellipse points towards the source [Summers, 1974]. The location of the ionospheric source may also be determined using the time delays associated with the arrival time of the wave front as it propagates over a network of ground stations [Althouse and Davis, 1978; Kemp, 1983]. A wavefront model that is plane, circular or elliptical may be used and between three and six stations are required. With the elliptical wave front model the number of stations may be reduced from six if a flat Earth is assumed and reliable polarization data is available to contribute to the source location.

The most conclusive way to estimate the reliability and accuracy of ground-based source location techniques is to relate the results to

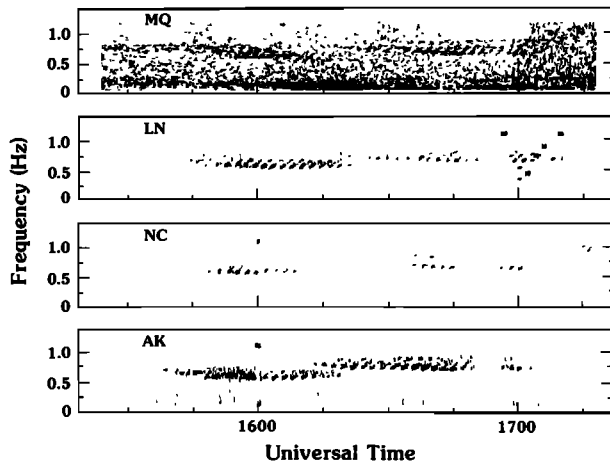


Fig. 1. A Pc 1 emission event recorded at four stations in Australasia between 1540-1710 UT on December 16, 1977. The stations are Macquarie Island (MQ,  $L = 4.3$ ) Launceston (LN,  $L = 2.7$ ), Newcastle (NC,  $L = 1.8$ ) and Auckland (AK,  $L = 1.9$ ).

direct observations of the primary source waves in the magnetosphere using spacecraft data. A preliminary comparison of a ground Pc 1 emission with the electron density profile from a radial outbound ISEE 1 pass identified a source region just inside a steep plasmopause [Fraser et al., 1984]. A more extensive study of this Pc 1 emission, including ISEE 1 electron density and ion composition data is reported in this paper.

Synchronous spacecraft studies by ATS 6 and GEOS 1 and 2 have shown that the presence of modest quantities of heavy ions ( $O^+$ ,  $He^+$ ) in the thermal plasma has a profound effect on the propagation of ion cyclotron waves in the magnetosphere. For example, in a two ion plasma ( $H^+$ ,  $He^+$ ) off-resonant absorption is seen near the  $He^+$  cyclotron frequency ( $f_{He^+}$ ) [Mauk, 1983] and a significant spectral slot due to a dispersion stop-band is seen between  $f_{He^+}$  and the LH wave mode cutoff frequency [Young et al., 1981; Fraser and McPherron, 1982]. A polarization reversal of the wave mode from LH to right-hand (RH) is seen at the crossover frequency. Similar effects are associated with the cyclotron cutoff and crossover frequencies introduced by the addition of thermal  $O^+$  ions [Fraser, 1982; Inhester et al., 1984; Fraser et al., 1986]. It is important to determine the effects of heavy ions on the ion cyclotron waves propagating to the Earth and observed by ground stations as Pc 1 emissions. Perraut et al. [1984] have shown that the large group of structured emissions seen on the ground are rarely seen at synchronous orbit, since they are generated at lower altitudes in the nighttime and morning plasmopause-plasmasphere sectors. It was noted that  $He^+$  propagation effects are not important since  $f_{He^+}$  is generally above the wave frequency. Fraser [1985] noted that although the  $O^+$  critical frequencies at these altitudes may occur in the Pc 1-2 band, no effects have been identified in structured pulsations seen on the ground. Results presented later show an example of a Pc 1 emission propagating at frequencies

between the equatorial critical frequencies of the  $O^+$  and  $He^+$  ions.

The properties of ion cyclotron waves considered so far relate to propagation effects. However, it is also important to consider the constraints placed on the wave spectrum by the proton cyclotron instability in a plasma containing both hot and cold multiple ion species. Detailed analysis of ATS 6 and GEOS wave spectra and anisotropic energetic proton distributions in the presence of low concentrations of  $He^+$  and  $O^+$  ions at synchronous orbit are generally consistent with linear growth rate theory [Mauk and McPherron, 1980; Roux et al., 1982; Inhester et al., 1984]. Linear convective growth rates have been calculated for the Pc 1 emission studied here and it will be shown that maximum growth occurs in the bandwidth where wave power is seen on the ground.

The following sections describe the analysis of a Pc 1 ion cyclotron wave event recorded on the ground by a network of recording stations in southeast Australia on December 16, 1977, between 1540-1710 UT. The Pc 1 activity is a classical example of a structured event of the type which occurs 3 to 5 days following major magnetic storm activity [Kawamura et al., 1982]. Also available are corresponding observations of plasma data from an outbound low-latitude ISEE 1 pass through the plasmopause region of the magnetosphere. This provides a unique opportunity to relate ground spectral observations with wave propagation and generation mechanisms in the magnetosphere.

#### Source Location

Pc 1 emission wave energy is propagated from a reasonably localized high latitude ionospheric secondary source region at the foot of the field line to middle and low-latitude stations in the ionospheric duct. It is assumed that the signal wave front expands outwards with time from this source region in a series of concentric ellipses. Observations of the wave polarization vector in the plane of the Earth may be used to locate the source of ducted emissions. If homogeneous plane waves propagate in the duct the major axis of a linearly polarized ellipse will indicate the group ray direction of arrival [Summers, 1974]. Horizontal propagation paths in the duct are traced taking into account refraction from  $f_oF_2$  gradients. This technique has been used by Webster and Fraser [1985] to locate the high-latitude source regions. With the source location known the wavefront ellipse parameters and group velocity may be calculated using the interstation time delays. These have been calculated and provide consistent results, but are not important in this study.

The dynamic spectra observed at four stations for the Pc 1 emission event to be studied are shown in Figure 1. A magnetic storm with maximum  $K_p = 5$  occurred on December 11, 1977, 5 days prior to the event. Magnetic activity was very quiet in the 24 hours preceding the event with  $\Sigma K_p = 8$ . Details of the station locations are given by Fraser [1976] and Webster and Fraser [1985]. Two discrete frequency bands are seen from 1540 to 1620 UT covering a frequency band 0.5-0.8 Hz and from 1612 to 1700 UT with a

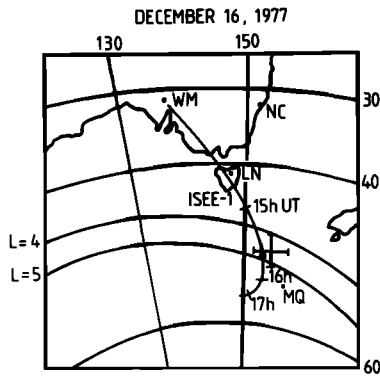


Fig. 2. The magnetic field line footprint for the outbound ISEE 1 orbit and the corresponding Pc 1 emission source location on December 16, 1977, between 1540 and 1620 UT. The solid circle on the ISEE orbit indicates the location of the plasmopause determined from the electron density profile.

bandwidth 0.7-0.9 Hz. For the present study the first event, over the time interval 1550-1615 UT, was analyzed in detail. The analysis techniques outlined above located the ionospheric source at

$51 \pm 3^\circ\text{S}$ ,  $156 \pm 4^\circ\text{E}$  geographic or  $L = 4.7 \pm 0.7$ . This location is plotted as crossed error bars in Figure 2.

#### ISEE 1 Observations

At the time of the Pc 1 emission event illustrated in Figure 1 the ISEE 1/2 spacecraft pair were outbound in the same local time sector at a latitude of  $25^\circ\text{N}$ . The footprint of the magnetic field line passing through the ISEE 1 orbit is plotted in Figure 2. The orbit intersects the error bars of the ground located source region at about 1525 UT. Data from the UCLA flux gate magnetometer experiment [Russell, 1978] were analyzed for wave activity between 1500 and 1700 UT, but no waves were seen above a noise level of 1 nT. This is not unexpected, since the ground observed emissions did not commence until 1540 UT, well after ISEE had passed through the source flux tube at 1525 UT.

The plasma environment over the 1500-1700 UT interval of this outbound ISEE 1 pass is summarized in the plots in Figure 3. The top plot shows the electron density data deduced from the University of Iowa plasma wave experiment (R.R. Anderson, private communication, 1987),

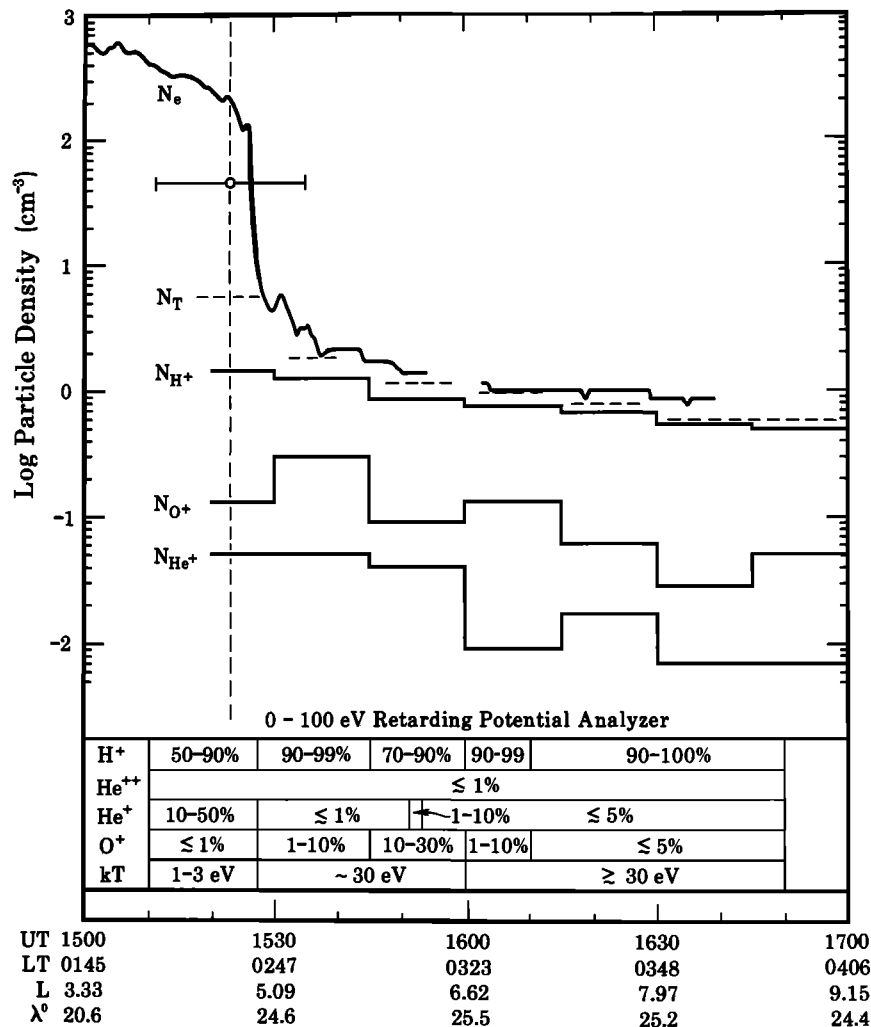


Fig. 3. The plasma environment observed by ISEE 1 in association with the Pc cyclotron wave emission. The vertical dashed line with error bars at  $L = 4.7$  indicates the radial location of the Pc 1 source.

which indicates a sharp plasmopause changing density from 150 to 4 cm<sup>-3</sup> over a range of 0.2 R<sub>E</sub> at L = 4.9. The time here is about 0300 LT and steep plasmopause gradients are typical during the early morning hours. The location of the Pc 1 emission source determined using ground-based measurements is indicated by the dashed vertical line with error bars at L = 4.7 ± 0.7. From the error range it can be seen that the source may be inside, on, or outside the plasmopause. However, wave packet bounce period results presented in the next section verify that the source must be in the high-density region, inside the plasmopause. The three lower plots, labeled N<sub>H</sub><sup>+</sup>, N<sub>O</sub><sup>+</sup> and N<sub>He</sub><sup>+</sup> indicate the densities of the 0.1-16 keV/e warm plasma constituents observed by the Lockheed retarding potential analyzer (RPA) and averaged over 20-min intervals (O.W. Lennartsson, private communication, 1987). The density N<sub>T</sub> (dashed bars) represents the total ion density in the energy range 0.01-16 keV/e. In the plasma trough (L > 5.0) this closely matches the sum of the 0.1-16 keV/e constituents plotted, indicating that there is very little <100 eV cool plasma in the trough which is a warm region. However, inside the plasmopause at L = 4.9 (~1520 UT) N<sub>T</sub> is well in excess of the sum of the warm constituents (0.1-16 keV/e) and is over an order of magnitude lower than N<sub>e</sub>. This indicates the presence of a cooler (10-100 eV) plasma and the predominance of a cool-cold (<10 eV) plasma in the plasmasphere. The tabulations at the bottom of Figure 3 show rough estimates of the 0-100 eV/e thermal ions from the RPA experiment. The various ions are indicated on the left and the estimates assume a flowing Maxwellian for each ion species. Precise values of number densities cannot be evaluated because of large and rapid fluctuations in both densities and flow velocities. In the plasmasphere around L = 4.9 the plasma is predominantly H<sup>+</sup> (50-90%) and He<sup>+</sup> (10-50%) with very little O<sup>+</sup> (<1%). The warm and cool plasma observations will be used in the following sections to model the ion cyclotron wave propagation and wave instability mechanisms for the Pc 1 emission event.

#### Wave Propagation

For ion cyclotron wave propagation the magnetosphere is considered a zero temperature neutral plasma containing electrons, protons, and He<sup>+</sup> and O<sup>+</sup> heavy ions. If the 0-100 eV ion relative concentrations in Figure 3 are considered representative of the cold plasma, which may not be unreasonable within the plasmasphere, then it is possible to calculate reasonably accurately the group travel time bounce period for the ion cyclotron wave packet propagation. This may then be compared with measured bounce periods which relate to the fine structure element spacing seen in the emissions in Figure 1.

The calculations are based on the method developed by Fraser [1972]. The group refractive index of the ion cyclotron wave takes the form

$$\mu'(\lambda, \beta, \gamma) = \mu_A \left| \frac{1 - \lambda/2}{(1 - \lambda)^2} - \frac{\beta(8\lambda - 4)}{(4\lambda - 1)^2} - \frac{\gamma(128\lambda - 16)}{16\lambda - 1} \right|$$

$$\cdot \left| \frac{1}{(1 - \lambda)} - \frac{4\beta}{(4\lambda - 1)} - \frac{16\gamma}{(16\lambda - 1)} \right|^{-1/2} \quad (1)$$

where  $\lambda$  is the wave frequency normalized to the proton cyclotron frequency,  $\beta$  the fractional He<sup>+</sup> ion concentration,  $\gamma$  the fractional O<sup>+</sup> ion concentration and  $\mu_A$  the refractive index at zero frequency in the absence of He<sup>+</sup> and O<sup>+</sup> ions ( $\beta = \gamma = 0$ ).

The double-hop transit time of an ion cyclotron wave packet bouncing between hemispheres is given by

$$T_G(\lambda, \alpha, \beta, \gamma) = 2/c \int_{\text{path}} \mu'(\lambda, \beta, \gamma) ds \quad (2)$$

where  $\alpha$  is the fractional concentration of the protons and  $\alpha + \beta + \gamma = 1$ . In order to undertake this integration a dipole field model is assumed with  $B = B_0 L^{-3}$  in the equatorial plane with  $B_0$  chosen to provide a main field magnitude agreeing with that measured by ISEE 1 at 24°N latitude and mapped back to the equator. A plasma density distribution model  $N = N_0 L^{-3}$  is used with  $N_0$  chosen to provide  $N$  which matches the measured electron concentration ( $N_e$ ) at L = 4.7. It is assumed that the ion and electron densities at the equator are the same as those measured by ISEE 1 off the equator. The major contribution to  $T_G$  occurs close to the equator and to avoid the singularities associated with the  $f_{He^+}$  and the O<sup>+</sup> cyclotron frequency  $f_{O^+}$  ( $\lambda = 0.25$  and 0.063) it is assumed that the He<sup>+</sup> and O<sup>+</sup> ions are confined to within latitudes ±10° of the equator. Beyond ±10° the plasma consists of only H<sup>+</sup> ions. The kernel of the integral in equation (2) maximizes in the equatorial region and therefore the major contribution to  $T_G$  occurs in this region. This has been shown for the analogous VLF whistler case by Carpenter and Smith [1964] and has also been used in Pc 1 wave propagation studies by Dowden [1966] and Fraser [1972]. Plots of the normalized travel time  $T_G/T_A$ , where  $T_A$  is the Alfvén (zero frequency) travel time, are shown in Figure 4. The He<sup>+</sup> and O<sup>+</sup> heavy ion concentrations used to plot Figure 4 were 8% He<sup>+</sup> with 1% O<sup>+</sup> (0.08, 0.01) and 10% He<sup>+</sup> with no O<sup>+</sup> (0.1, 0). The dispersion curve for a pure H<sup>+</sup> plasma (0,0) is also plotted. The He<sup>+</sup> concentrations chosen represent the lower end of the measured 10-50% contribution indicated by the cool ions in Figure 3. It will be shown later that this He<sup>+</sup> concentration provides the best agreement with experimental results. There are two nonpropagation stop bands indicated in Figure 4, one between  $f_{O^+}$  and the O<sup>+</sup> cutoff frequency, and the other between  $f_{He^+}$  and the He<sup>+</sup> cutoff frequency [Young et al., 1981; Fraser and McPherron, 1982]. Since parallel propagation is assumed, there is no crossover of wave modes.

It is now of interest to compare the dispersion results in Figure 4, which indicate allowed propagation bands and expected normalized travel times, with experimental data determined from the wave properties shown in Figure 1. The computed  $T_G$  travel times should relate to the fine structure element spacing seen in the wave spectra, which is a measure of the wave packet

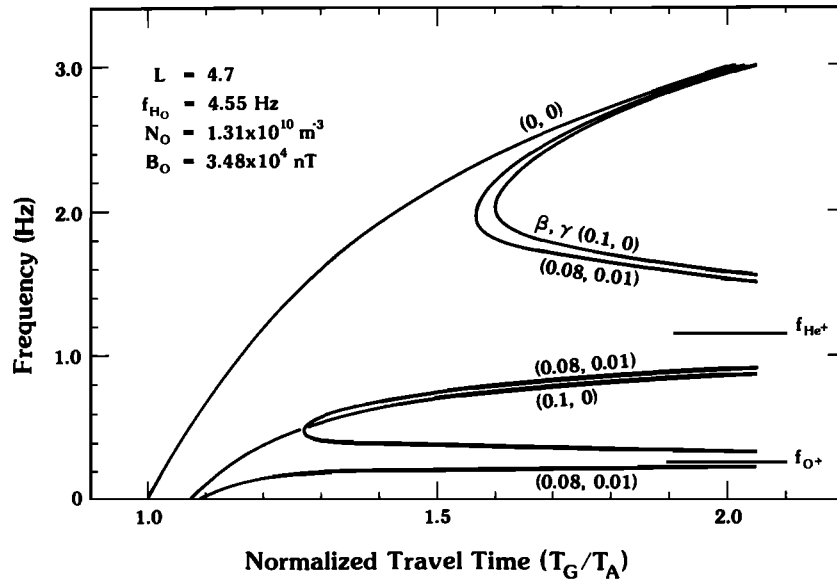


Fig. 4. Dispersion curves for LH mode ion cyclotron wave propagation along the field line in a multiple ion plasma. The relative fractional concentrations and  $O^+$  ( $\beta, \gamma$ ) are given in parenthesis.

double-hop bounce period. The measured bounce periods for the four stations over the 1553-1609 UT interval were determined using envelope detection and spectral analysis techniques described by Samson [1983] and are plotted in Figure 5 over this time interval and in a bandwidth 0.57-0.69 Hz. The bounce period ( $T_G$ ) shows a systematic increase with time at all stations from 140 s to 155 s. Increases in  $T_G$  with time may indicate that the wave source is slowly drifting to higher L shells [Fraser, 1968] or is stationary but associated with a changing plasma density with time. However, a change in

plasma density over such a short time may not be expected since the plasmopause region is stable in this early morning local time sector [Higel and Lei, 1984]. The segments of the dispersion curves from Figure 4 over the 0.4-0.8 Hz frequency band between  $f_{O^+}$  and  $f_{He^+}$  are plotted in Figure 6. Superimposed on this figure is a box showing the range of experimentally measured bounce periods  $\Delta T_G = 155-140$  s over a bandwidth  $\Delta f = 0.69-0.57$  Hz. It should be remembered that the overall emission bandwidth was 0.5-0.8 Hz over the considered time interval. The wave packet bounce periods calculated from dispersion theory with concentrations of 8 and 10%  $He^+$  and 0 and 1%  $O^+$  agree well with the measured bounce periods. With a fixed  $O^+$  concentration of 1% the minimum and maximum limits placed on the  $He^+$  concentration by the box are 6% and 12%. The significance of these results will be considered in the discussion section.

#### Ion Cyclotron Wave Generation

In addition to the wave propagation effects in the magnetosphere which determine the spectra seen on the ground there are also constraints provided by the generating instability. The convective growth rate of ion cyclotron waves is calculated using the plasma data at  $L = 4.7$  from Figure 3 in the analytical expressions derived by Gomberoff and Neira [1983]. The modifications by Kozyra et al. [1984] to include bi-Maxwellian anisotropic distributions in the energetic multiple ion components are also taken into consideration. The cold populations, including electrons, are described by Maxwellian distributions with thermal velocities ( $v_{th,j}$ ) which satisfy  $\Omega_j/v_{th,j} k \gg 1$  where  $\Omega_j$  is the cyclotron frequency of component  $j$ .

The linearized dispersion relation for the LH ion cyclotron mode propagating parallel to the ambient magnetic field  $B_0$ , is given by [Kozyra

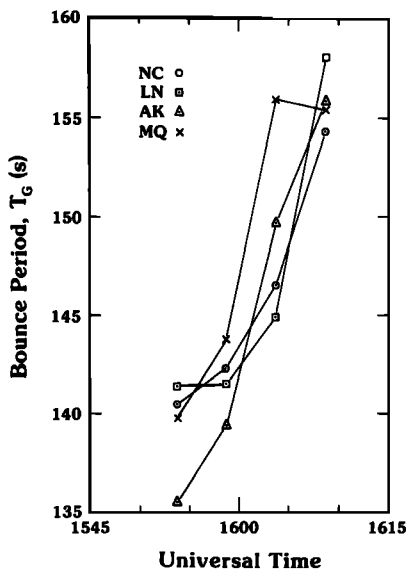


Fig. 5. Experimentally determined ion cyclotron wave packet group bounce period. Data relates to the fine structure element spacing in the 0.57-0.69 Hz bandwidth slice through the dynamic spectra shown in Figure 1.

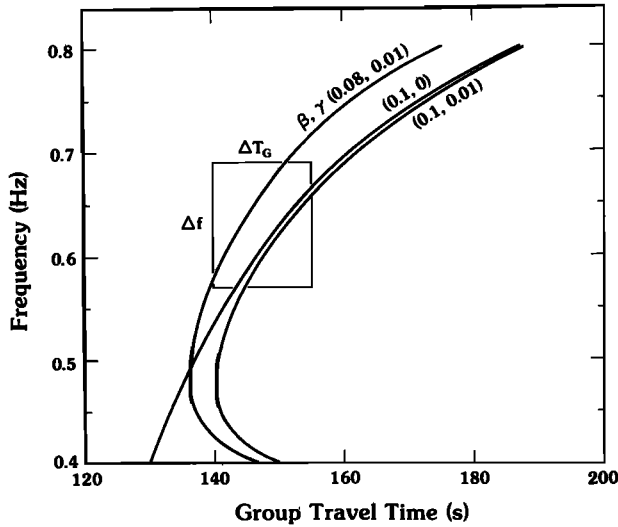


Fig. 6. A section of the dispersion curves in Figure 4 for the frequency range 0.4-0.8 Hz. Also shown is the  $\Delta f$ ,  $\Delta T_G$  box defined by the experimental results with  $\Delta f = 0.69$ -0.57 Hz and  $\Delta T_G = 155$ -140 s.

et al., 1984, equation (2)]

$$\omega^2 = c^2 k^2 - \sum_{\ell} \omega_{p\ell w}^2 \left\{ A_{\ell} - \frac{Z(\xi_{\ell})}{\alpha_{\ell}} [(A_{\ell} + 1)(\Omega_{\ell} - \omega) - \Omega_{\ell}] \right\} + \sum_j \omega_{pj c}^2 \frac{\omega}{\omega - \Omega_j} \quad (3)$$

where  $\omega_{p\ell w(c)}$  is the plasma frequency of species  $\ell$ ,  $w(c)$  indicates the warm (cold) component, the thermal anisotropy is given by  $A_{\ell} = (T_{\perp \ell} / T_{\parallel \ell}) - 1$ , the parallel thermal velocity by  $\alpha_{\ell}$ , and  $Z(\xi_{\ell})$  is the plasma dispersion function. The summation over the cold components  $j$  includes the electrons and over  $\ell$  relates to the energetic species.

Assuming  $\omega = \omega_r + i\omega_i$  ( $\omega_r \gg \omega_i$ ) the convective growth rate is given by

$$\gamma_s = \frac{\mu}{V_g} = \left\{ \sum_{\ell} \frac{\eta_{\ell w} \sqrt{\pi}}{M_{\ell}^2 \alpha_{\ell}} [(A_{\ell} + 1)(1 - M_{\ell} X) - 1] \cdot \exp \left[ \frac{-\eta_{\ell w} (M_{\ell} X - 1)^2}{M_{\ell}^2 \beta_{\ell w} X^2} \right] \right. \\ \left. \cdot \left[ \frac{(1 + \delta)}{(1 - X)} + \sum_j \frac{(\eta_{jw} + \eta_{jc}) M_j}{1 - M_j X} \right] \right\} \\ \cdot \left\{ 2X^2 \left[ \frac{(1 + \delta)}{(1 - X)} + \sum_i (\eta_{iw} + \eta_{ic}) \frac{M_i}{1 - M_i X} \right] \right\}^{-1} \quad (4)$$

where  $V_g$  and  $k$  are given by the real part of the dispersion relation,  $X = \omega_r / \Omega_p$ , and  $M_{\ell} = m_{\ell} / z m_p$ . The summation over  $\ell$  includes  $H^+$ ,  $He^+$  and  $O^+$  and over  $i$  and  $j$  only the heavy ions  $He^+$  and  $O^+$ . A detailed discussion of the growth rate theory has

been given by Kozyra et al. [1984] and will not be included here. Experimental parameters required to calculate  $\gamma_s$  are the ratio of the concentration of each hot and cold species to the hot protons ( $\eta_{\ell}$ ), the cold to hot relative proton concentration ( $\delta$ ), and anisotropy ( $A_{\ell}$ ) and perpendicular temperature ( $T_{\perp \ell}$ ) for each species. The cold and warm heavy ion data from Figure 3 inside the plasmopause at  $L = 4.7$  are listed in Table 1. The unknown parameters needed to calculate the growth rates are  $A_{\ell}$  and  $T_{\perp \ell}$  for each ion species. Parameter studies indicate that growth rates and their frequency bands are relatively unaffected by changes in  $A(He^+, O^+)$  over the range 0-3 and  $T_{\perp}(He^+, O^+)$  over the range 5-30 keV for the small hot  $He^+, O^+$  concentrations present (Table 1). Thus, the arbitrary choice of  $T_{\perp}(He^+, O^+)$  at 10 keV is reasonable. This is supported by recent ring current heavy ion studies which show greatest  $He^+$  and  $O^+$  fluxes at  $\leq 20$  keV energies during the storm recovery phase [Krimigis et al., 1985]. The hot proton energy is chosen from typical synchronous orbit data [Mauk and McPherron, 1980; Roux et al., 1982; Inhester et al., 1984] and theoretical modeling [Criswell, 1969]. The 0-16 keV proton concentration used in Table 1 is assumed to represent the hot  $T_{\perp}(H^+) = 30$  keV protons. However, there may be variations in  $H^+$  concentration with energy [Gloeckler et al., 1985]. Parameter studies show for an order of magnitude change in  $H^+$  concentration the growth rate increases by an order of magnitude but the frequencies over which growth occurs are essentially unchanged. Results are shown in Figure 7, where convective growth rates are plotted, in units of  $\omega_i / V_g$ , as a function of frequency. The hatched region between 0.5-0.8 Hz indicates the bandwidth of the Pc 1 emission observed on the ground. It can be seen that the growth rate increases as the anisotropy of the hot protons increases. The widest spectrum of wave amplitude is seen in the broad peak in the growth rate between  $f_{0+}$  and  $f_{He+}$  which corresponds to the emission band seen on the ground. The sharp peak below  $f_{0+}$  is of low amplitude, and this may account for its absence in the ground spectra. The peak in the growth rate above  $f_{He+}$  is somewhat unstable and essentially collapses for hot proton anisotropies  $A \leq 0.75$ .

It is important to define the regime over which the analytical expression for the

TABLE 1. Parameters Used in Convective Growth Rate Calculations

Particles	$H^+$	$He^+$	$O^+$
Cold, $cm^{-3}$	196	22	2
Warm, $cm^{-3}$	5.1	0.05	0.13
$T_{\perp \ell}$ , keV	30	10	10
$A_{\ell}$	0.75, 1.0, 1.5	1	1

$$|B| = 300 \text{ nT}; N_e = 220 \text{ cm}^{-3}.$$

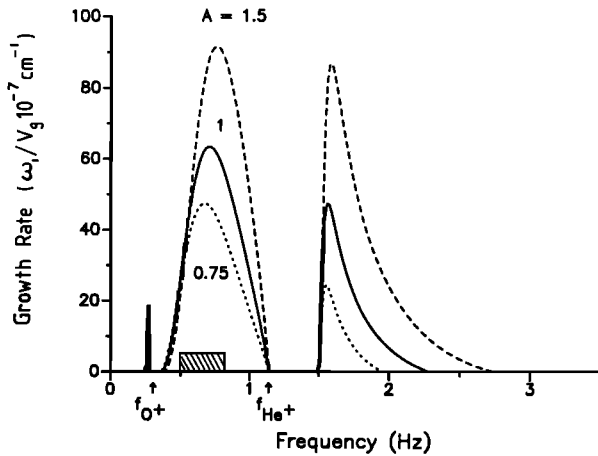


Fig. 7. Linear convective wave growth calculations for the plasma parameters listed in Table 1. The hatched area indicates the band of Pc 1 frequencies observed by the ground stations.

convective instability in equation (4) is valid. Recently, Oscarsson and Andre [1986] noted that the approximations used by Gomberoff and Neira [1983] are not valid if the instability becomes non-convective. The regions of absolute and convective instabilities for plasmas containing 0% and 15%  $\text{He}^+$  are illustrated by Roux et al. [1982, Figure 12]. Here  $\beta_i$ , the ratio of the kinetic to the magnetic pressure is plotted against  $A_{H^+}$ . From the data in Table 1 for the energetic protons  $N_{H^+} = 5 \text{ cm}^{-3}$ ,  $T_{L,H^+} = 30 \text{ keV}$  and  $B = 300 \text{ nT}$ , and using  $\beta_{L,H^+} = N_{H^+} T_{L,H^+} / (B^2 / 2\mu_0)$  yields  $\beta_{L,H^+} = 0.67$ . Roux et al. [1982, Figure 12] shows the instability will be convective provided  $A_{H^+} < 1.5$  for  $f < f_{\text{He}^+}$ . To comply with this constraint the level of anisotropy has been limited to 1.5 in Figure 7.

#### Discussion and Conclusions

It has been shown that the source of a structured Pc 1 ion cyclotron emission event is in the high-density plasmasphere at  $L = 4.7 \pm 0.7$ , just inside a steep plasmapause at  $L = 4.9 \pm 0.1$ . An associated ISEE 1 outbound pass identified signal amplitudes of 1 nT at the same frequency but the spacecraft magnetometer data could not be analyzed because of spin contamination. However, ISEE 1 plasma data providing the electron and warm (0.1-16 keV/e) and cool (<100 eV/e)  $\text{H}^+$ ,  $\text{He}^+$  and  $\text{O}^+$  ion density radial profiles were available. These data were used to determine the dispersive propagation characteristics of an ion cyclotron wave packet bouncing between hemispheres along the  $L = 4.7$  field line in a multicomponent plasma. The bounce periods were found to agree with those measured experimentally from the Pc 1 emission fine structure element spacing (Figure 1) provided the  $\text{He}^+$  and  $\text{O}^+$  concentrations were about 10% and 1%, respectively.

The concentration of 10%  $\text{He}^+$  is at the low end of the 10-50% range suggested from the 0-100 eV/e cool  $\text{He}^+$  RPA results in Figure 3. There are a number of arguments that can be suggested to support a lower  $\text{He}^+$  concentration than that

indicated by the RPA experiment. Firstly, the ISEE 1 0-100 eV/e measurements may not truly represent the cold plasma density. There may be a cold population which is not seen because of the shielding provided by spacecraft charging [Olsen, 1982]. Charging is a particular problem where the spacecraft is ramming the plasmapause and the high density plasmasphere. Also, in the presence of convection produced by wave fields measurement of the relative abundances of heavy ions from particle detectors are difficult [Mauk, 1982]. Therefore a lower  $\text{He}^+$  fractional concentration of 10% may not be unreasonable.

As the ion cyclotron wave packet propagates down the field line from the equator into an increasing ambient field there will be a location where, for zero wave normal angle, the wave will have a frequency matching the local  $\text{O}^+$  cutoff frequency and will cease to propagate unless the local  $\text{O}^+$  relative concentration is very low. Then wave tunneling may occur [Dowden, 1966] and wave energy will propagate to the ionosphere and the ground. If the wave normal angle is nonzero, then a polarization reversal will occur where the wave frequency matches the local  $\text{O}^+$  crossover frequency. The wave then becomes RH polarized and is not affected by the  $\text{O}^+$  cyclotron resonance and will continue to be guided until it matches the local bi-ion frequency and is reflected [Young et al., 1981]. Provided the  $\text{O}^+$  concentration is smaller than a few percent, the waves may tunnel through this reflection region [Perraut et al., 1984]. In this situation a field aligned duct may be required to guide the RH mode wave energy down to the ionosphere and the ground. Here the double-hop transit time will no longer be completely described by equation (2). Directly under the source, RH polarization may be expected. In the present ground data, MQ is situated nearest the source (Figure 2) at a distance between 0 and 600 km, and LH elliptical polarization was observed throughout the wave event. The more distant lower latitude stations showed linear or mixed linear and RH polarization which is more typical for ionospherically ducted signals. Therefore it would appear that the waves undergoing a polarization reversal in the magnetosphere at the  $\text{O}^+$  crossover frequency are not seen on the ground near the source. Alternatively, if parallel propagation is assumed in the magnetosphere then the LH and RH waves are decoupled. As noted previously in the absence of a crossover some of the LH ion cyclotron wave packet energy may tunnel through the cyclotron resonance region. Again, this is most likely to occur when  $\text{O}^+$  concentrations are only a few percent, a situation which is satisfied here with  $\approx 1\%$  of  $\text{O}^+$  ions. This may explain the observation of LH waves at MQ. With higher  $\text{He}^+$  densities tunneling above  $f_{\text{He}^+}$  is not possible and this may contribute to the lack of waves on the ground at  $f > f_{\text{He}^+}$ .

The linear convective growth rate calculations, undertaken using the cool and warm  $\text{H}^+$ ,  $\text{He}^+$  and  $\text{O}^+$  data provided by the ISEE 1 data at  $L = 4.7$  and an assumed free energy source of energetic protons, indicate largest broadband growth rates over the frequencies seen in the emission observed on the ground. Also worthy of consideration is the error associated with the source region determination of  $L = 4.7 \pm 0.7$ .

Since the plasmopause is at  $L = 4.9$  this does not eliminate the possibility that the source may be in the low-density trough region immediately outside the plasmopause. However, calculation of ion cyclotron wave packet group travel times using the ISEE 1 plasma data for this region gives  $T_G = 18-20$  s which is not a realistic time considering the experimental bounce periods measured were 140-155 s. Furthermore, convective wave growth calculations in this region show very small amplitudes in the Pc 1 emission frequency band observed.

In summary, this study provides a consistent description of ion cyclotron wave packets generated by the proton cyclotron instability propagating along a field-aligned path in the plasmasphere just inside the plasmopause and transmitting energy into the  $F_2$  region ionospheric duct. The duct then distributes the wave energy over a wide area to ground stations. This integrated result has been made possible by the use of the ground polarization source location technique to determine the wave packet propagation field line. The most convincing result is the agreement of ground wave packet bounce periods, measured from dynamic spectra, with those calculated independently for parallel wave propagation using ISEE 1 plasma data. Also, simple linear convective wave growth calculations show significant wave amplitudes over the emission band observed.

**Acknowledgments.** Thanks are due to C. T. Russell for providing the ISEE 1 magnetometer data, W. Lennartsson and R. R. Anderson for ISEE 1 plasma data and R. L. McPherron and J. C. Samson for helpful discussions. This work was supported by the Australian Research Grants Scheme. Part of the work was undertaken while one of the authors (B.J.F.) was on study leave at UCLA, and R. L. McPherron is thanked for support during this time.

The Editor thanks J. U. Kozyra and another referee for their assistance in evaluating this paper.

#### References

- Althouse, E. L., and J. R. Davis, Five station observations of Pc 1 micropulsation propagation, *J. Geophys. Res.*, **83**, 132, 1978.
- Carpenter, D. L., and R. L. Smith, Whistler measurements of electron density in the magnetosphere, *Rev. Geophys.*, **2**, 415, 1964.
- Criswell, D. R., Pc 1 micropulsation activity and magnetospheric amplification of 0.2-5.0 Hz hydromagnetic waves, *J. Geophys. Res.*, **74**, 205, 1969.
- Dowden, R. L., Micropulsation nose whistlers: A helium explanation, *Planet. Space Sci.*, **14**, 1273, 1966.
- Feigen, F. Z., J. P. Kurchashov, V. A. Troitskaya, D. S. Fligel, and K. Dobes, Method of locating the Pc 1 source and hot plasma parameters in the generation region, *Planet. Space Sci.*, **27**, 151, 1979.
- Fraser, B. J., Temporal variations in Pc 1 geomagnetic micropulsations, *Planet. Space Sci.*, **16**, 111, 1968.
- Fraser, B. J., Propagation of Pc 1 micropulsations in a proton-helium magnetosphere, *Planet. Space Sci.*, **20**, 1883, 1972.
- Fraser, B. J., Pc 1 geomagnetic pulsation source regions and ionospheric waveguide propagation, *J. Atmos. Terr. Phys.*, **38**, 1141, 1976.
- Fraser, B. J., Pc 1 observations of heavy ion effects by synchronous satellite ATS-6, *Planet. Space Sci.*, **30**, 1229, 1982.
- Fraser, B. J., Observations of ion cyclotron waves near synchronous orbit and on the ground, *Space Sci. Rev.*, **42**, 357, 1985.
- Fraser, B. J., and R. L. McPherron, Pc 1-2 magnetic pulsation spectra and heavy ion effects at synchronous orbit, *J. Geophys. Res.*, **87**, 4560, 1982.
- Fraser, B. J., W. J. Kemp, and D. J. Webster, Pc 1 pulsation source regions and their relationship to the plasmopause, Proceedings of Conference on Achievements of the IMS, *Eur. Space Agency Spec. Publ.*, **ESA SP-217**, 609, 1984.
- Fraser, B. J., J. C. Samson, R. L. McPherron, and C. T. Russell, Ion cyclotron waves observed near the plasmopause, *Adv. Space Res.*, **6**, 223, 1986.
- Gendrin, R., S. Lacourly, A. Roux, J. Solomon, F. Z. Feigen, M. V. Gokhberg, V. A. Troitskaya, and V. L. Yakimenko, Wave packet propagation in an amplifying medium and its application to the dispersion characteristics and to the generation mechanisms of Pc 1 events, *Planet. Space Sci.*, **19**, 165, 1971.
- Gloeckler, G., B. Wilkin, W. Studeman, F. M. Ipavich, D. Hovestadt, D. C. Hamilton, and G. Kremser, First composition measurement of the bulk of the storm-time ring current (1-300 keV/e) with AMPTE/CCE, *Geophys. Res. Lett.*, **12**, 325, 1985.
- Gomberoff, L., and R. J. Neira, Convective growth rate of ion cyclotron waves in a  $H^+-He^+$  and  $H^+-He^+-O^+$  plasma, *J. Geophys. Res.*, **88**, 2170, 1983.
- Hayashi, K., T. Kokubun, T. Oguti, K. Tsuruda, S. Machida, T. Kitamura, O. Saka, and T. Watanabe, The extent of Pc 1 source region in high latitudes, *Can. J. Phys.*, **59**, 1097, 1981.
- Higel, B., and W. Lei, Electron density and plasmopause characteristics at 6.6  $R_E$ : A statistical study of the GEOS 2 relaxation sounder data, *J. Geophys. Res.*, **89**, 1583, 1984.
- Inhester, B., V. Wedeken, A. Korth, S. Perraut, and M. Stokholm, Ground-satellite coordinated study of the April 5, 1979, *J. Geophys.*, **55**, 134, 1984.
- Kawamura, M., M. Kuwashima, and T. Toya, Comparative study of magnetic Pc 1 pulsations observed at low and high latitudes: Source region and generation mechanism of periodic hydromagnetic emissions, Proceedings of 4th Symposium on Coordinated Observations of the Ionosphere and Magnetosphere in Polar Regions, *Mem. Natl. Inst. Polar Res., Spec. Issue*, **22**, 3, 1982.
- Kemp, W. J., Multistation observations of Pc 1 geomagnetic pulsations at middle and low latitudes, Ph.D. thesis, Univ. of Newcastle, New South Wales, Australia, 1983.
- Kennel, C. F., and H. E. Petscheck, Limit on stably trapped particle fluxes, *J. Geophys. Res.*, **71**, 1, 1966.



- Kozyra, J. U., T. E. Cravens, A. Nagy, and E. G. Fonthelm, Effects of energetic heavy ions on electromagnetic ion cyclotron wave generation in the plasmopause region, J. Geophys. Res., **89**, 2217, 1984.
- Krimigis, S. M., G. Gloeckler, R. W. McEntire, T. A. Potemra, F. L. Scarf, and E. G. Shelley, Magnetic storm of Sept. 4, 1984: A synthesis of ring current spectra and energy densities measured with AMPTE/CCE, Geophys. Res. Lett., **12**, 329, 1985.
- Manchester, R. N., Correlation of Pc 1 micropulsations at spaced stations, J. Geophys. Res., **73**, 3549, 1968.
- Mauk, B. H., Helium resonance and dispersion effects on geostationary Alfvén/ion cyclotron waves, J. Geophys. Res., **87**, 9107, 1982.
- Mauk, B. H., Frequency gap formation in electromagnetic cyclotron wave distribution, Geophys. Res. Lett., **10**, 635, 1983.
- Mauk, B. H., and R. L. McPherron, An experimental test of the electromagnetic ion cyclotron instability within the earth's magnetosphere, Phys. Fluids, **23**, 2111, 1980.
- Olsen, R. C., The hidden ion population of the magnetosphere, J. Geophys. Res., **87**, 3481, 1982.
- Oscarsson, T., and M. Andre, Waves with frequencies below the proton gyrofrequency in a multicomponent plasma, Ann. Geophys., **4**, 319, 1986.
- Perraut, S., Wave-particle interactions in the ULF range: GEOS-1 and -2 results, Planet. Space Sci., **30**, 1219, 1982.
- Perraut, S., R. Gendrin, A. Roux, and D. Villedary, Ion cyclotron waves: Direct comparison between ground-based measurements and observations in the source region, J. Geophys. Res., **89**, 195, 1984.
- Roux, A., S. Perraut, J. L. Rauch, D. de Villedary, G. Kremser, A. Korth, and D. T. Young, Wave-particle interactions near  $\Omega_{He}^+$  observed on board GEOS 1 and 2, 2, Generation of ion cyclotron waves and heating of  $He^+$  ions, J. Geophys. Res., **87**, 8174, 1982.
- Russell, C. T., The ISEE 1 and 2 fluxgate magnetometers, IEEE Trans. Geosci. Electron., **GE-16**, 239, 1978.
- Samson, J. C., Pure states, polarized waves and principle components in the spectra of multiple geophysical time series, Geophys. J. R. Astron. Soc., **72**, 647, 1983.
- Summers, W. R., Production mechanisms for the observed behaviour of the low latitude Pc 1 polarization ellipse, Planet. Space Sci., **22**, 801, 1974.
- Webster, D. J., and B. J. Fraser, Source regions of low latitude Pcl pulsations and their relationship to the plasmopause, Planet Space Sci., **33**, 777, 1985.
- Young, D. T., S. Perraut, A. Roux, D. de Villedary, R. Gendrin, A. Korth, D. Kremser, and D. Jones, Wave-particle interactions near  $\Omega_{He}^+$  observed on GEOS 1 and 2, 1, Propagation of ion cyclotron waves in a  $He^+$  rich plasma, J. Geophys. Res., **86**, 6755, 1981.

B.J. Fraser, and D.J. Webster. Department of Physics, University of Newcastle, New South Wales, 2308, Australia.

W.J. Kemp, CSIRO, Division of Environmental Mechanics, Institute of Physical Sciences, Canberra, Australian Capital Territory, 2601, Australia.

(Received April 25, 1988;  
revised May 1, 1989;  
accepted May 3, 1989.)